miR-338-3p inhibits A549 lung cancer cell proliferation and invasion by targeting AKT and β-catenin signaling pathways

JIA LIU[1], LINGGAI CAO[1], NA ZHAO[1], YUE FENG[1], ZE YU[1], YUHUA LI[1], CHUNBO TENG[1], JIFAN HU[2] and TAO LI[1]

[1]Department of Genetics, College of Life Science, Northeast Forestry University, Harbin, Heilongjiang 150040, P.R. China; [2]Department of Basic Science, Stanford University Medical School, Palo Alto Veterans Institute for Research, Palo Alto, CA 94305, USA

Received January 10, 2018; Accepted January 17, 2019

DOI: 10.3892/mmr.2019.10215

Abstract. The aim of the present study was to explore the underlying mechanism of microRNA-338-3p (miR-338-3p) in lung cancer cell (A549) invasion and proliferation. A microarray assay showed that miR-338-3p upregulated 216 and downregulated 147 genes in A549 cells, and the differentially expressed genes were enriched for several signaling pathways, including AKT and β-catenin signaling pathways. Western blotting results showed that phosphorylated (p)-AKT at Ser473 and at Thr308 and p-β-catenin at Ser552 were downregulated. Inhibiting AKT signaling pathway decreased β-catenin signaling pathway. Overexpression of β-catenin promoted the invasion of A549 cells. In addition, miR-338-3p showed inhibitory effect on the primary tumor developed from $Kras^{G12D}$ mice. Together, the data of the present study support that miR-338-3p inhibits lung cancer cell invasion and proliferation by downregulating AKT/β-catenin signaling pathway. The present findings supported the potential use of miR-338-3p in the treatment of lung cancer.

Introduction

Lung cancer, which originates from the bronchial epithelium, is one of the most malignant diseases, with high rates of morbidity and mortality (1). Among them, the non-small cell lung cancer (NSCLC) prevalence is 80%, but the 5-year survival is only ~15%, while the small cell lung cancer has survival rates of 15-20%. Only 16% of patients with lung cancer can be diagnosed at an early stage, and lung cancer metastasis is the major reason for ineffective treatment and patient mortality (1-3). Metastasis to different organs could occur at later stages of lung cancer progression, which often results in the patient experiencing profound pain and having an increased risk of mortality (4).

MicroRNA (miRNA/miR)s have been shown to be efficient regulators in a variety of disease models and thus, are proposed to have great potential in therapeutic applications (5). miR-338-3p exerts negative effects on the proliferation of neuroblastoma cells, and it could also inhibit the migration and invasion of human neuroblastoma cells, which involves direct targeting of the 3' untranslated region of phosphhatidylinoitol-3,4,5-trisphosphate dependent Rac exchange factor 2a mRNA while it affects the Phosphatase and Tensin homolog (PTEN)/Akt signaling pathway (6). The phosphoinositide 3 kinase (PI3K)/AKT signaling pathway is involved in the invasion of squamous cell carcinoma (7-10), while the association between miR-338-3p and AKT signaling pathway, the role of PI3K/AKT and its downstream signaling pathway in lung cancer cell invasion lacks further investigation. miR-338-3p is capable of suppressing cell proliferation and of inducing apoptosis of non-small-cell lung cancer, suppressing epithelial-mesenchymal transition (EMT) and metastasis in lung cancer cells (11,12). An RNA-Seq assay may help to get a better profile of the impact of miR-338-3p on lung cancer cells. Furthermore, the suppressing effect of miR-338-3p on lung cancer cells proliferation needs to be evaluated in an *in vivo* model.

About 30% of human tumors carry a mutation of ras gene (13-15). Of the three genes in this family (composed of K-ras, N-ras and H-ras), K-ras is the most frequently mutated member in human tumors, including adenocarcinomas of the pancreas and the lung (16,17). $Kras^{G12D}$ mice were used in the present study as an *in vivo* tumor model, to investigate the efficiency of miR-338-3p on tumor inhibition, *in vivo*.

To further elucidate the role of miR-338-3p in inhibiting lung cancer cell invasion, *in vitro* and *in vivo* assays were performed in the present study. The results of the present study demonstrated that miR-338-3p inhibited lung cancer cell invasion and proliferation by downregulating the AKT/β-catenin signaling pathway. This finding partially determined the underlying mechanism of the inhibitory role of miR-338-3p on lung cancer cell invasion and proliferation. Additionally, these data supported the potential use of miR-338-3p in the treatment of lung cancer.

Correspondence to: Dr Tao Li, Department of Genetics, College of Life Science, Northeast Forestry University, Yifu Building, 26 Hexing Street, Harbin, Heilongjiang 150040, P.R. China
E-mail: taoliharb@163.com

Key words: A549, AKT, invasion, microRNA-338-3p

Materials and methods

Cell culture, transfection and apoptosis assay. The A549 cell line was purchased from the American Type Culture Collection (Manassas, VA, USA). The cells were cultured in Dulbecco's modified Eagle's medium (Invitrogen; Thermo Fisher Scientific, Inc., Waltham, MA, USA) containing 10% fetal bovine serum (Invitrogen; Thermo Fisher Scientific, Inc.) and were maintained at 37˚C in an atmosphere containing 5% CO_2 and 95% humidity. Cell apoptosis was determined using an Annexin V-FITC Apoptosis Detection Kit I (BD Biosciences, Franklin Lakes, NJ, USA) with a FACS Influx flow cytometer (BD Biosciences) according to the manufacturer's protocol. Briefly, cells were re-suspended in a pre-cooled staining buffer and the cell density was adjusted to $2x10^7$ cells/ml. Then 50 μl (~10^6 cells) of cell suspension was transferred to a 1.5 ml Eppendorf tube and 300 μl of 1X Binding Buffer was added. Subsequently, 5 μl of Annexin V-FITC was added to the tube and incubated at room temperature for 15 min. Finally, 5 ml of PI reagent was added for 5 min at room temperature before analysis. The cells were suspended with the appropriate amount of 1X Binding buffer and the staining results were analyzed by flow cytometry within 30 min. In all flow cytometry assay, 10,000 events were analyzed by flow cytometry (BD Biosciences) using CellQuest™ Pro software (version 5.1; BD Biosciences).

miR-338-3p mimic (miR-338-3p) and corresponding miRNA negative control (miR-NC) were transfected into A549 cells using Lipofectamine® 2000 (Invitrogen; Thermo Fisher Scientific, Inc.) according to the manufacturer's protocol. In total, 100 nmol/l miR-338-3p mimics was used for transfection at a cell confluence of 50-60%. The cells were analyzed 24-48 h after the transfection. The microRNA was synthesized by Sangon Biotech Co., Ltd. (Shanghai, China). The microRNA sequences were as follows: miR-338-3p mimics: 5'-AACAAUAUCCUGGUGCUGAGUG-3'; negative control mimics: 5'-UUCUCCGAACGUGUCACGUTTACG UGACACGUUCGGAGAATT-3'.

Reverse transcription-quantitative polymerase chain reaction (RT-qPCR). For the RT-qPCR analyses of miR-338-3p expressions, total RNA of tissues and cells was extracted using TRIzol® RNA reagent (Invitrogen; Thermo Fisher Scientific, Inc.), and first-strand cDNA was prepared via RT with Superscript II reverse transcriptase (Invitrogen; Thermo Fisher Scientific, Inc.). The RT-PCR sample was incubated at 42˚C for 50 min and heated to inactivate the enzyme at 70˚C for 15 min. The expression of miR-338-3p was quantified using Fast SYBR Green Master Mix (Applied Biosystems; Thermo Fisher Scientific, Inc.) under ABI 7300 Sequence Detection System (Life Technologies; Thermo Fisher Scientific, Inc.), according to the manufacturer's protocol and normalized to the expression of U6. The primers were as follows: Forward (F)-miR-338-3p (5'-TGCGGTCCA GCATCAGTGAT-3') and reverse (R)-miR-338-3p (5'-CCA GTGCAGGGTCCGAGGT-3'), F-U6 (5'-TGCGGGTGCTCG CTTCGGCAGC-3') and R-U6 (5'-CCAGTGCAGGGTCCG AGGT-3'). The PCR temperature protocol was set as follows: The sample was incubated for 30 min at 16˚C, followed by 60 cycles at 30˚C for 30 sec, 42˚C for 30 sec and 50˚C for 1 sec, and incubated at 85˚C for 5 min to inactivate the reverse transcriptase. The relative expression of each gene was calculated and normalized by the $2^{-\Delta\Delta Cq}$ method (18). Each sample was tested in triplicate.

Reagents. Perifosine (AKT inhibitor; 2.5 μM for 24 h at 37˚C), LY294002 (PI3K inhibitor; 0.5 μM for 24 h at 37˚C), BIO (GSK-3 inhibitor; 2.5 μM for 24 h at 37˚C) XAV939 (Wnt/β-catenin signaling inhibitor; 30 nM for 24 h at 37˚C) were purchased from Selleck.cn (Selleck Chemicals, Houston, TX, USA). The compound bpV was purchased from BioVision (PTEN inhibitor; BioVision, Inc., Milpitas, CA, USA). The cell invasion assay was conducted using 24-well Transwell chambers with 8 μM pores (Corning, Inc., Corning, NY, USA). In total, $1x10^5$ cells in Dulbecco's modified Eagel's medium (DMEM; Thermo Fisher Scientific, Inc.) without serum were added to the Matrigel-coated chambers, and 1 ml DMEM was added to the bottom chamber. A small amount of serum (0.5% fetal bovine serum; Biological Industries, Kibbutz Beit Haemek, Israel) was added to bottom of the chamber to stimulate cell invasion. Following incubation for 24 h, the filters were fixed (4% paraformaldehyde; 15 min at room temperature) and stained with 0.2% crystal violet (10 min at room temperature). Invaded cells were manually counted in five random fields under a light microscope (Olympus Corporation, Tokyo, Japan), and images (magnification, x200) were captured.

Proliferation assay. An MTT assay was used to analyze cell proliferation. A549 cells were transfected with either miR-338-3p mimic (miR-338-3p) or mimic control (NC). After 24 h transfection, cells were seeded into 96-well plate at $5.0x10^3$ cells/ml and cultured for 24 h. At each time point, 10 μl MTT reagent (5 mg/ml; Sigma-Aldrich; Merck KGaA) was added to each well, successive incubated for 4 h at 37˚C. The supernatant was removed and 200 μl DMSO (Invitrogen; Thermo Fisher Scientific, Inc.) was added to dissolve the formazan crystals for 30 min. Spectrometric absorbance at a wavelength of 570 nm was measured on microplate reader (Spectra Max M5; Molecular Devices, LLC, Sunnyvale, CA, USA). Each sample was tested in triplicate and all experiments were performed three times.

Animal model. Primary lung cancer was induced in $Kras^{G12D}$ mice as previously described (19). Briefly, 7-8-week-old mice (C57/B6 background; n=6; female; weight, 20±2 g, kept at a temperature of 21±2˚C, with free access to water/food and kept in a 8/16 dark/light cycle) were anaesthetized with diethyl ether and received 64 μl of cre-advenovirus (AdCre) solution (Biowit Technologies, Ltd., Shenzen, China) through the nasal cavity. The virus solution was prepared by mixing 30 μl of AdCre (10^{10} pfu), 70 μl of Eagle's minimum essential medium (Sigma-Aldrich; Merck KGaA), and 0.5 μl of 2 M $CaCl_2$ and placed in room temperature for 20 min. The weight of mice was determined every two days. Subsequently, 35 days after the virus treatment, the mice were euthanatized via CO_2 (in a 3 L chamber for 3 min), the lung tissues were harvested, and their size and weight were determined. All procedures were performed with the approval of the Animal Ethics Committee of Shenzhen Jiake Biotechnology Co., Ltd. (Shenzhen, China).

Lung cancer tissues were washed with PBS and fixed with 4% paraformaldehyde (12 h at room temperature), and the sections were paraffin-embedded, cut into 6 μm sections, and stained with routine H&E. The sections were deparaffinized with xylene for 10 min at room temperature and rehydrated in absolute alcohol for 5 min, 95% alcohol for 2 min and 70% alcohol for 2 min. The sections were briefly washed in distilled water and stained in Harris hematoxylin solution for 8 min at room temperature. Subsequently, the sections were washed in running tap water for 5 min and differentiated in 1% acid alcohol for 30 sec. The sections were washed with running tap water for 1 min, placed in 0.2% ammonia water for 30 sec, washed in running tap water for 5 min and rinsed in 95% alcohol. The sections were counterstained in eosin-phloxine B solution for 30 sec at room temperature, followed by dehydration with 95% alcohol, two changes of absolute alcohol, 5 min each. They were cleared in xylene for 5 min and mounted with xylene based mounting medium. The sections were visualized using a light microscope (magnification, x200; CKX53; Olympus Corporation).

In vivo delivery of miR-338-3p. A mPEG-PLGA-PLL-LA (PEAL-LA; Sigma-Aldrich; Merck KGaA) nanoparticle-based microRNA *in vivo* delivery was applied as previously described (20). One nanomole of miR-338-3p was dissolved in 50 μl RNase-free water and emulsified in 500 μl dichloromethane solution containing 5 mg of PEAL-LA copolymer by sonication (Scientz sonicator probe, Ningbo Scientz Biotechnology, Co., Ltd., Zhejiang, China) at 400 W for 1 min on ice to obtain a water/oil emulsion. Subsequently, 2 ml PluronicTM F68 water solution (1 mg/ml) was added to the water/oil emulsion and sonicated again to obtain a water/oil/water emulsion. The resulting water/oil/water emulsion was transferred to a rotary evaporator (150 g; 20˚C) to evaporate the organic solvent and obtain the miR-338-3p-PEAL-LA nanoparticles. One week following AdCre administration in $Kras^{G12D}$ mice, a single dose of miR-338-3p-PEAL-LA nanoparticles (at a dose of 0.53 mg/kg miR-338-3p) formulated above were administered via tail vein injection every 2 days for 4 weeks.

Microarray assay. For the microarray assay, total RNA of tissues and cells ($1x10^6$ at a confluence of 95%) was extracted using TRIzol® RNA reagent (Invitrogen; Thermo Fisher Scientific, Inc.) and RNA was reversed to cDNA with a cDNA RT kit (Agilent Technologies, Inc., Santa Clara, CA, USA). The RT sample was incubated at 42˚C for 50 min and heated to inactivate the enzyme at 70˚C for 15 min. A total of 10 μg of labeled cRNA was hybridized at 45˚C for 16 h to the mouse genome array MOE430A2.0 (Affymetrix; Thermo Fisher Scientific, Inc.). Processed chips were read with an Agilent G2565CA Microarray Scanner (Agilent Technologies, Inc.). Scanned microarray images were imported into GeneSpring GX (v12.0) software to generate signal values and absent/present calls for each probe-set using the MAS 5.0 statistical expression algorithm; this process identified genes that were differentially expressed.

Immunofluorescence. Cells (at the confluence of 80-90%) were fixed with 4% formaldehyde for 15 min at room temperature and permeabilized with 0.2% (v/v) Triton X-100 in PBS for 10 min at room temperature. Specimens were incubated with anti-Ki67 (cat. no. GTX16667; 1:100; GeneTex, Inc., Irvine, CA, USA), anti-serine-473-AKT (cat. no. GTX121936; 1:100; GeneTex, Inc.) and anti-β-catenin antibodies (cat. no. GTX101254; 1:100; GeneTex, Inc.) at 4˚C overnight and then incubated with Alexa Fluor-488/Cy3-conjugated anti-rabbit IgG at 37˚C for 1.5 h (cat. nos. 406416 and 406402; 1:200; BioLegend, Inc., San Diego, CA, USA). To stain the nuclei, the specimens were incubated with DAPI solution (2.5 mg/ml^{-1}; Sigma-Aldrich; Merck KGaA, Darmstadt, Germany) for 10 min at room temperature. The fluorescence signal was visualized using a confocal microscope (magnification, x600; Olympus Corporation).

Western blotting (WB). Subconfluent cell cultures were washed with D-PBS, and cell lysates were prepared in a lysis buffer containing 1% (v/v) Triton X-100, 1% (v/v) deoxycholic acid, 2 mM $CaCl_2$ and protease inhibitors (10 μg/ml leupeptin, 10 μg/ml aprotinin, 1.8 mg/ml iodoacetamide and 1 mmol/l phenylmethyl sulfonyl fluoride) and quantified using a bicinchoninic protein assay kit (Pierce; Thermo Fisher Scientific, Inc.). Equal amounts of total protein (30 μg whole cell lysate) were subjected to electrophoresis on 12% Bis/Tris gels, transblotted onto nitrocellulose membranes, and probed with different primary antibodies. The membranes were blocked for 1 h at room temperature using blocking buffer containing 3% bovine serum albumin (BSA; Sigma-Aldrich; Merck KGaA) in PBS. Primary antibodies for AKT (cat. no. GTX121936), β-catenin (cat. no. GTX101254), phosphorylated (p)-β-catenin (Ser33/47/Thr41; cat. no. GTX132605), p-β-catenin (Ser45; cat. no. GTX50180), p-β-catenin (Ser675; cat. no. GTX123611), AKT (Ser473; cat. no. GTX128414), p-AKT (Thr308; cat. no. GTX28933), E-cadherin (cat. no. GTX100443), intercellular adhesion molecule-1 (ICAM-1; cat. no. GTX64322), matrix metalloproteinase-1 (MMP-1; cat. no. GTX100534), MMP-2 (cat. no. GTX104577), GAPDH (cat. no. GTX100118) were purchased from GeneTex, Inc. and p-β-catenin (Ser552; cat. no. 956; Cell Signaling Technology, Inc., Danvers, MA, USA) were all diluted (1:1,000) with blocking agent and applied to membranes for 24 h at 4˚C. Membranes were washed with PBST and incubated with horseradish peroxidase (HRP)-conjugated secondary antibodies (1:200; cat. no. sc-2357; Santa Cruz Biotechnology, Inc., Dallas, TX, USA) for 2 h at room temperature and washed with PBST. A chemiluminescent detection (Thermo Fisher Scientific, Inc.) of HRP activity was used to detect the signal in the membranes, and images were taken with chemiluminescence apparatus (Quantity One® software; Bio-Rad Laboratories, Inc., Hercules, CA, USA).

Statistical analysis. Each experiment was repeated at least three times independently. The results are expressed as the mean ± standard error, unless stated otherwise. Statistical comparisons among multiple groups were conducted using one-way analysis of variance with the Student-Newman-Keuls test, or a Student's t-test (unpaired, two-tailed) was used when making comparisons between two groups. $P<0.05$ was considered to indicate a statistically significant difference.

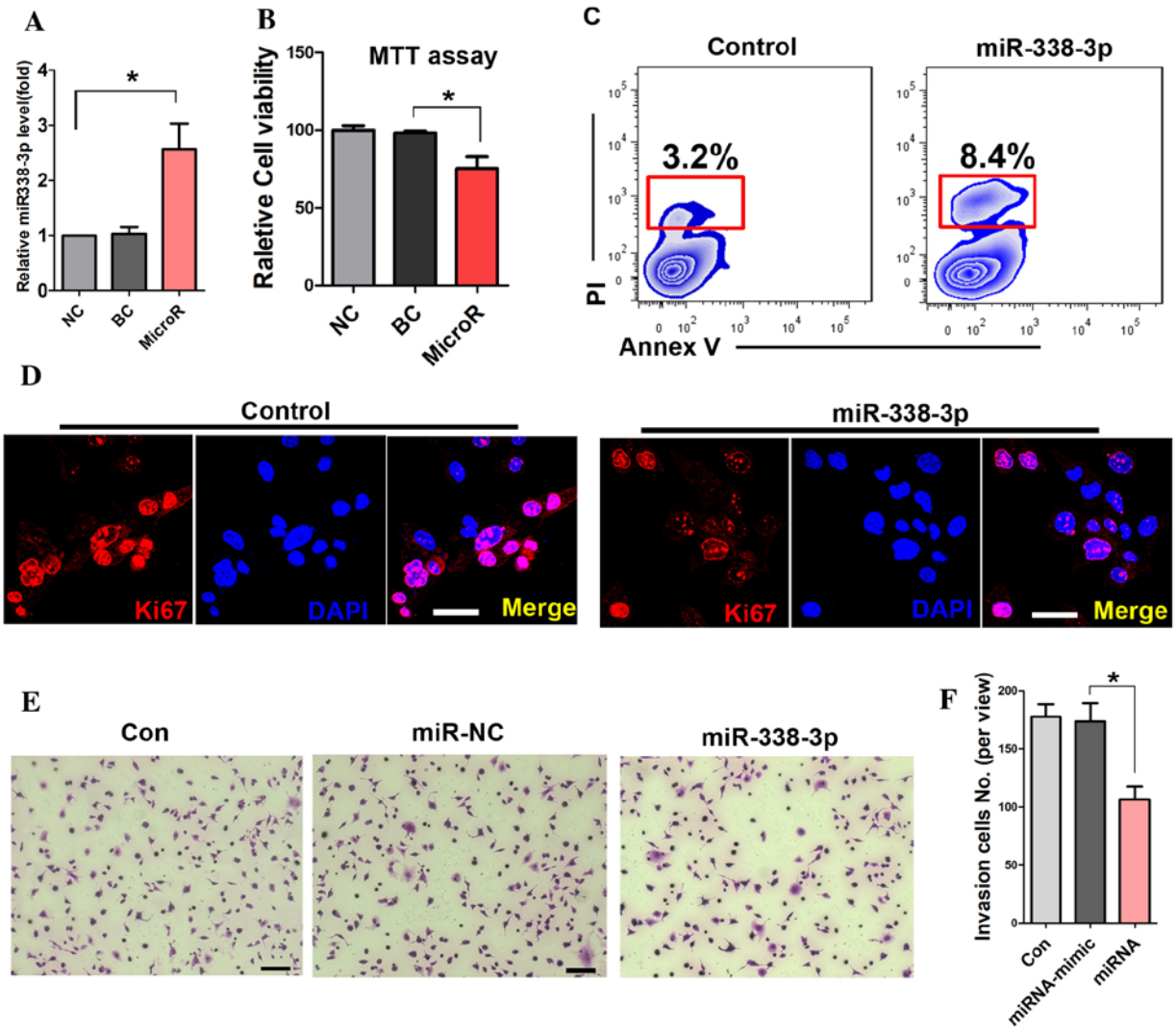

Figure 1. miR-338-3p inhibits the proliferation and invasion of A549 cells. (A) miR-338-3p expression levels were significantly increased in the miR-338-3p transfected cells compared with the control groups. (B) MTT assay of A549 cell viability in the miR-338-3p-treated group and the control group. (C) Cell apoptosis analysis with flow cytometry. The apoptotic cells were carefully gated via the relevant control cells. (D) Immunostaining of Ki67 in cells administered different treatments. Scale bar, 20 μm. (E) Cell invasion assay and (F) quantitation *P<0.05. Scale bar: 50 μm. BC, blank control; miR, microRNA; NC, negative control.

Results

miR-338-3p inhibits the proliferation and invasion of A549 cells. To detect the transfection efficiency of miR-338-3p, RT-PCR was performed. The result showed that miR-338-3p expression levels were significantly increased in the miR-338-3p transfected cells (Fig. 1A). The MTT assay showed that miR-338-3p attenuated the viability of A549 cells (Fig. 1B). Further cell apoptotic analysis with flow cytometry showed that miR-338-3p enhanced the apoptotic rate of A549 cells compared with that in the miR-NC group (8.4 and 3.2%; Fig. 1C). In addition, the expression of Ki67 was significantly reduced in miR-338-3p-treated cells (Fig. 1D). Furthermore, the number of migrated cells in the transwell assay was significantly reduced in the miR-338-3p-treated group during the cell invasion assay (Fig. 1E and F).

The effect of miR-338-3p on the transcriptome of A549 cells. A microarray assay was performed to evaluate the effect of miR-338-3p on the A549 cell transcriptome, and the bioinformatic analysis result showed that 216 genes were upregulated and 147 genes were downregulated in miR-338-3p-treated cells (Fig. 2A and B). Further bioinformatics analysis indicated that these altered genes were enriched in several signaling pathways, including the Janus kinase-signal transducer and activator of transcription, PI3K/AKT and Wnt signaling pathways (Fig. 2C).

miR-338-3p downregulates AKT and β-catenin signaling pathways. To further evaluate the effect of miR-338-3p on AKT and β-catenin signaling pathway, immunostaining and WB were performed. First, immunostaining showed that the expression levels of (p-AKT at Ser473) were reduced in miR-338-3p cells (Fig. 3A), and similar results were observed in the β-catenin staining (Fig. 3B). The WB results showed that both p-AKT(Ser473) and p-AKT(Thr308) were downregulated with miR-338-3p treatment (Fig. 3C), while p-β-catenin (Ser552) but not p-β-catenin (Ser33/47/Thr41), p-β-catenin (Ser45) or p-β-catenin (Ser675) was downregulated (Fig. 3D). In addition,

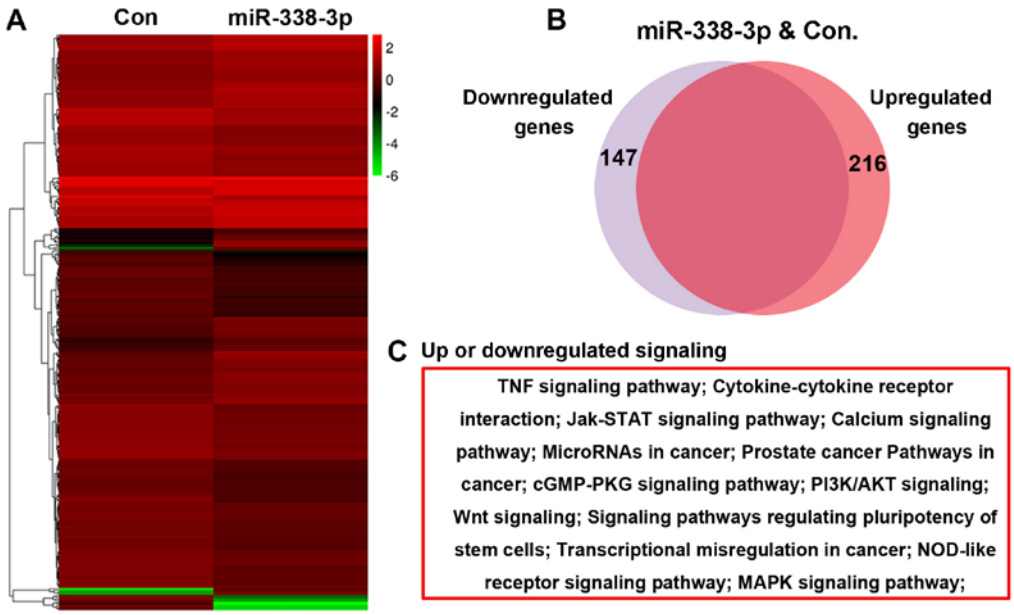

Figure 2. The effect of miR-338-3p on the transcriptome of A549 cells. (A and B) Microarray assay showing that 216 genes were upregulated and 147 genes were downregulated in miR-338-3p-treated cells. (C) KEGG analysis showing the differentially expressed genes that were enriched for several signaling pathways, including the Jak-signal transducer and activator of transcription, PI3K/AKT and Wnt signaling pathways. cGMP-PKG, cyclic guanosine monophosphate-protein kinase G; Con, control; MAPK, mitogen-activated protein kinase; miR, microRNA; PI3k, phosphoinositide 3-kinase; TNF, tumor necrosis factor.

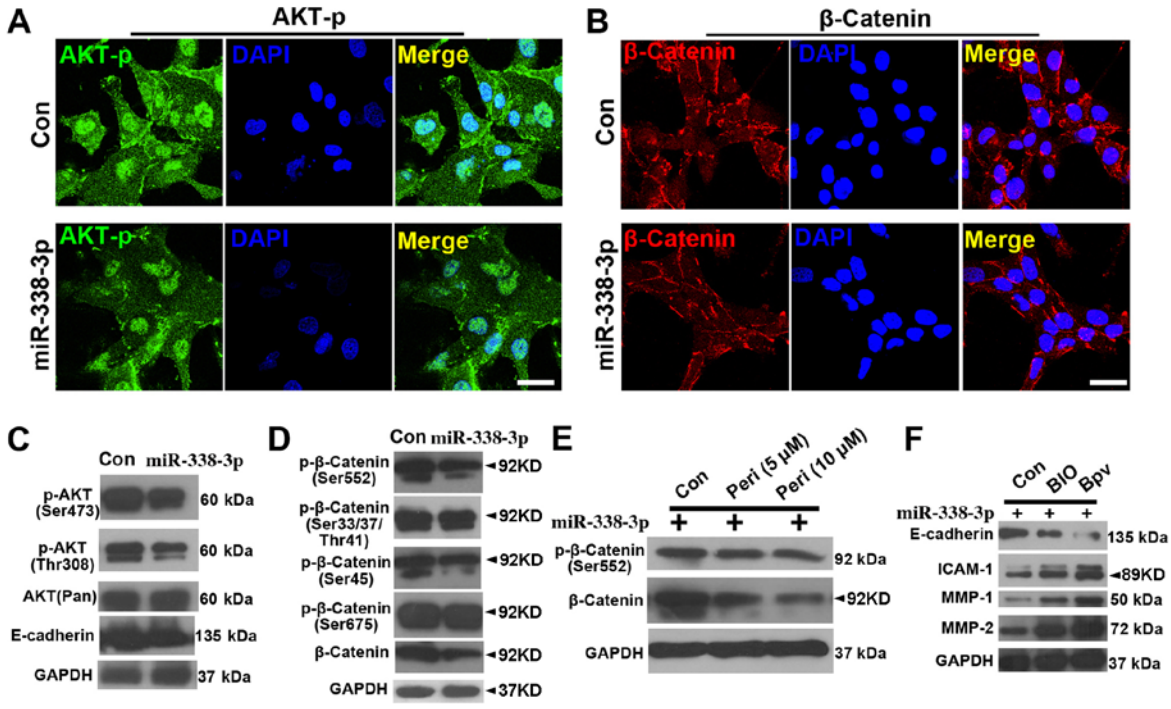

Figure 3. miR-338-3p downregulates AKT and β-catenin signaling pathway. Phosphorylated (Ser473) AKT (p-AKT) is reduced in miR-338-3p-treated cells (A), and (B) similar result was observed in the β-catenin staining. Western blotting results show that (C) both p-AKT(Ser473) and p-AKT (Thr308) were downregulated with miR-338-3p treatment, while (D) only p-β-catenin (Ser552), but not p-β-catenin (Ser33/47/Thr41), p-β-catenin (Ser45) or p-β-catenin (Ser675), was downregulated. (E) Inhibition of AKT signaling pathway with perifosine attenuated the activity of both p-β-catenin (Ser552) and β-catenin. (F) A decrease in E-cadherin expression levels and an increase in ICAM-1, MMP-1 and MMP-2 expression levels, in miR-338-3p-treated A549 cells after treatment with BIO and bpV. Scale bar, 20 μm. Con, control; ICAM, intercellular adhesion molecule; miR, microRNA; MMP, matrix metalloproteinase; Peri, perifosine.

inhibiting AKT signaling with perifosine attenuated the activity of both p-β-catenin (Ser552) and β-catenin (Fig. 3E), suggesting that AKT signaling positively regulated β-catenin signaling. Further assay of the expression of cell invasion markers showed that activation of both β-catenin (with BIO) and AKT (with bpV) signaling in miR-338-3p-treated A549 cells resulted in a

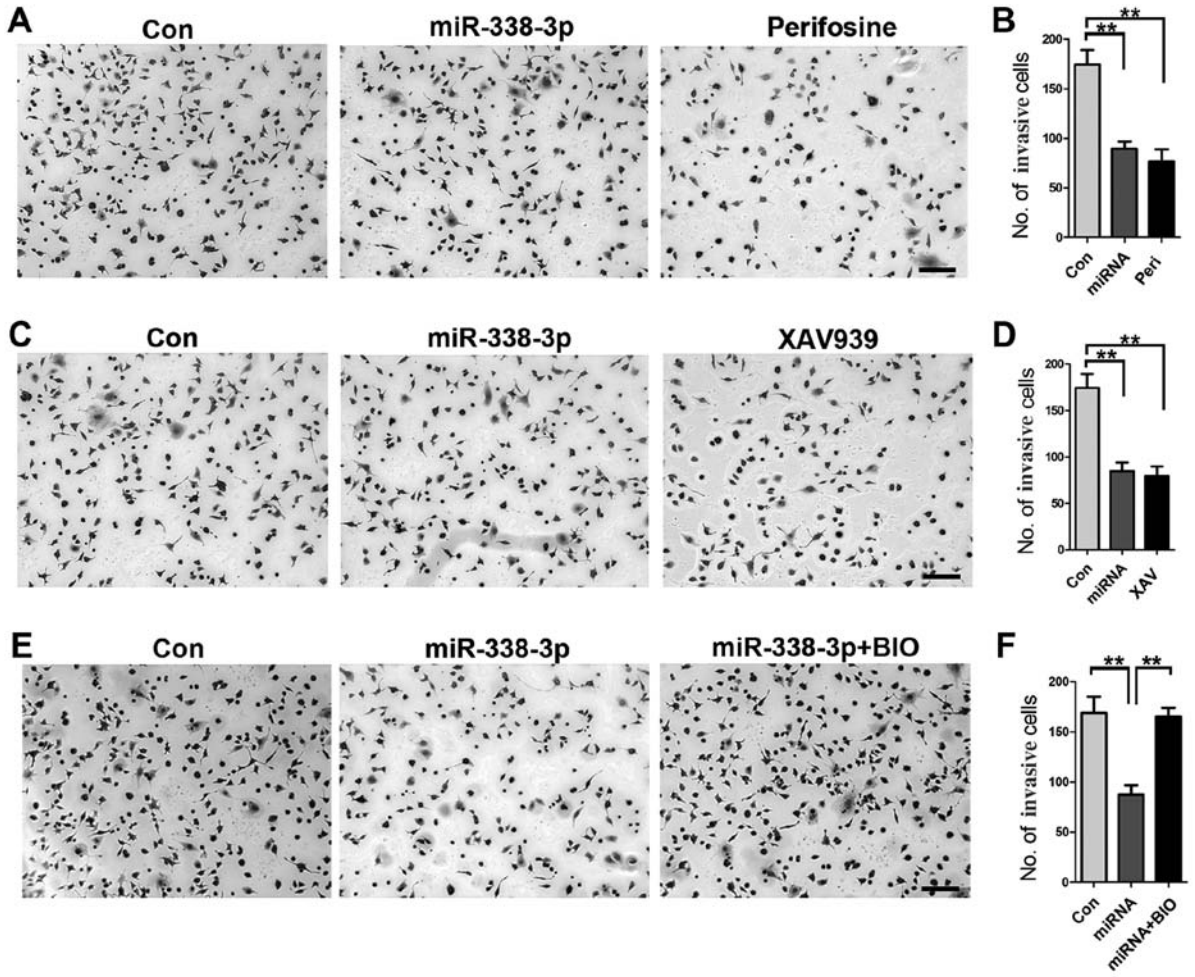

Figure 4. AKT and β-catenin signaling pathways serve crucial roles in miR-338-3p-mediated inhibition of A549 cell invasion (A and B) Inhibition of AKT signaling with perifosine resulted in a significant reduction of the number of invasive cells. (C and D) Inhibition of β-catenin signaling pathway with XAV939 resulted in an extensive decrease in invasive A549 cells. (E and F) Increased activity of β-catenin with BIO could rescue the inhibitory effect of miR-338-3p on A549 cell invasion. $^{**}P<0.01$. Scale bar, 50 μm. Con, control; miR, microRNA; Peri, perifosine.

decrease in E-cadherin expression and an increase in intercellular adhesion molecule-1, matrix metalloproteinase (MMP)-1 and MMP-2 expression (Fig. 3F).

AKT and β-catenin signaling serve crucial roles in miR-338-3p-inhibited A549 cell invasion. To gain further insight into the role of AKT and β-catenin signaling pathways in how miR-338-3p inhibits A549 cell invasion, a cell invasion assay was performed. First, inhibition of AKT signaling pathway with perifosine resulted in a significant reduction of invasive cells (Fig. 4A and B); similarly, inhibition of β-catenin signaling with XAV939 resulted in decreased number of invasive cells (Fig. 4C and D), indicating the important role of both AKT and β-catenin signaling pathways in miR-338-3p-mediated inhibition of A549 cell invasion. Furthermore, increased activity of β-catenin with BIO rescued the inhibitory effect of miR-338-3p on A549 cell invasion (Fig. 4E and F), validating the crucial role of AKT/β-catenin signaling pathway in miR-338-3p-induced inhibition of A549 cell invasion.

miR-338-3p inhibits lung cancer development in vivo. To investigate the efficiency of miR-338-3p on tumor inhibition, *in vivo*, a lung cancer model in $Kras^{G12D}$ mice was established, in which the cre-advenovirus (AdCre) was administrated via nasal cavity $Kras^{G12D}$ mice (Fig. 5A). Lung cancer was developed within five weeks after AdCre treatment, H&E staining showed malignant cell hyperproliferation in the AdCre treated tissue (Fig. 5B). To test the efficiency of miR-338-3p in this primary lung cancer model, the *in vivo* miR-338-3p delivery system was applied via mPEG-PLGA-PLL-LA nanoparticles. The result showed that following the continuous treatment of miR-338-3p for four weeks, the tumor weight on the 35th day after the primary tumor initiation was decreased in the miR-338-3p treated group compared with the control groups (Fig. 5C). To further evaluate the role of miR-338-3p on modulating AKT and β-catenin signaling pathways, western blotting on the lung tissue in different treated group was performed. Phosphorylation of β-catenin was analyzed to determine the underlying mechanism of the upregulation of β-catenin, and it was identified that β-catenin (ser552) was the phosphorylation peptide. For this experiment, the total expression level of β-catenin was assessed to evaluate the change of Wnt/β-catenin. The result showed that both the AKT-p and β-catenin expression levels were reduced in the miR-338-3p treated group (Fig. 5D and E). Although the total AKT level was slightly decreased in the miR-338-3p treated group, the AKT-p was significantly reduced, thus miR-338-3p

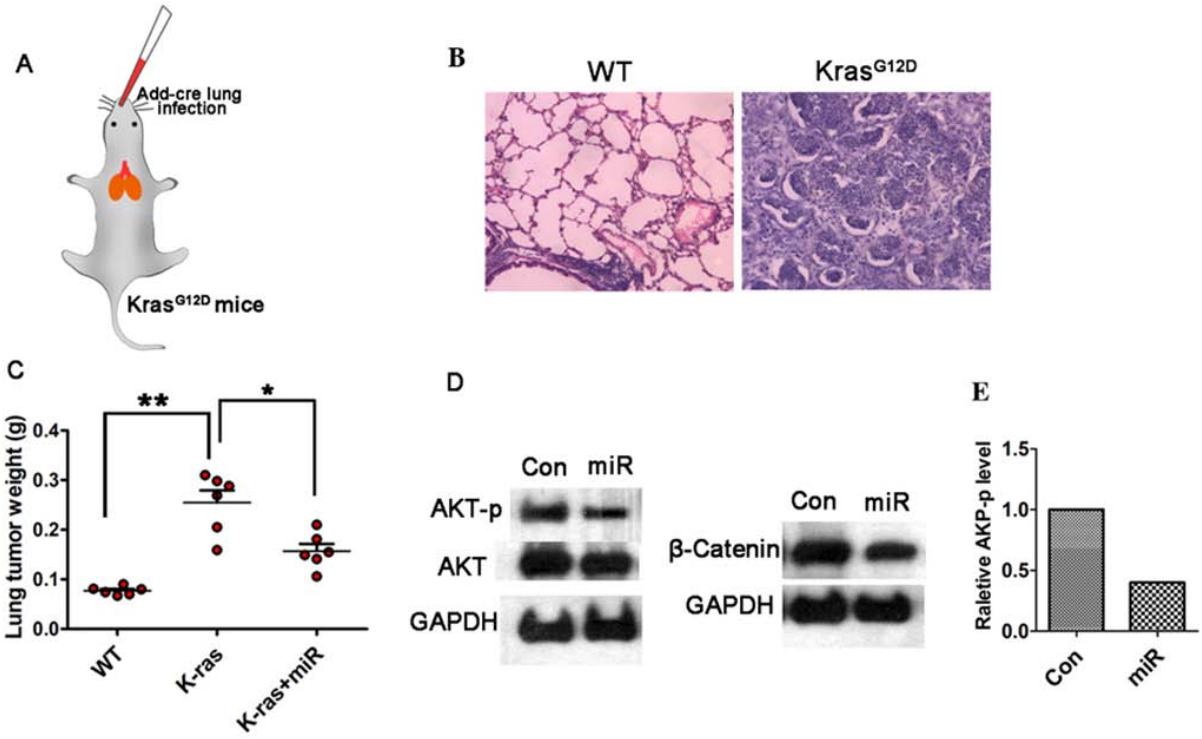

Figure 5. miR-338-3p inhibits lung cancer development *in vivo*. (A) Schematic of lung cancer model with nasal cavity treatment of cre-advenovirus (AdCre) in KrasG12D mice. (B) H&E staining showing malignant cell hyperproliferation in AdCre treated tissue. (C) Tumor weights on the 35th day after the primary tumor initiation are decreased in the miR-338-3p treated group compared with the control groups $^{*}P<0.05$, $^{**}P<0.01$. (D) AKT-p and total protein level of β-catenin was reduced in the miR-338-3p treated group. (E) Quantification of the relative AKT-p expression levels. Con, control; miR, microRNA; p, phosphorylated; WT, wild-type.

may efficiently reduce AKT signaling; however, this requires further investigation. These data support that miR-338-3p is capable to suppress AKT and β-catenin signaling pathway in lung cancer *in vivo*. Taken together, the present data indicate that miR-338-3p may inhibit A549 lung cancer cell proliferation and invasion by targeting AKT and β-catenin signaling, *in vitro* and *in vivo*.

Discussion

The most common clinical metastases are lung cancer (21). The recurrence and metastasis of lung cancer are complicated processes with multiple steps involving the degradation of tumor extracellular matrix, the enhancement of the invasive ability of tumor cells, tumor neovascularization and other cell biological behaviors. Some contributors to these processes include changes in gene expression and associated gene regulation, molecular signal pathway abnormalities (22,23).

A previous study has shown that EMT is associated with tumor invasion, tumor metastasis and drug resistance (24). Therefore, a novel tumor treatment strategy target for EMT was established in a previous study (25). MicroRNAs serve a regulatory role in human gene expression, and abnormal tumor expression and microRNA regulation extensively affect the development of the tumor. Inhibition of EMT-associated miRNAs in the tumor results in the abatement of tumor invasion and metastasis; however, promoting the expression of EMT-associated miRNAs accelerate tumor development. Although a small number of miRNAs have been identified by biochemical or bioinformatics methods, more studies were needed to investigate the biological functions of them and to develop a systematic understanding of their roles in tumor development and metastasis.

Accumulating data support Akt promote the growth and proliferation of tumor cells, inhibit cell apoptosis, increase hypoxia tolerance of cells via phosphorylating various downstream substrates (26,27). Invasion, metastasis, and promotion of resistance to chemotherapy and radiotherapy of cancer cells are linked with overexpression and activation of AKT in a variety of tumor tissues (28). p-AKT occurs during AKT activation and AKT1 is one of the important subtypes of AKT, and its expression is also increased in human gastric cancer (29). Abnormal expression and activity of AKT1 are also found in breast cancer, serving an important role in its metastasis (30). The data of the present study indicated that miR-338-3p is capable to inhibit the metastasis of lung cancer cells, *in vitro*, in which the AKT signaling was a crucial mediator. Additionally, the data of the present study supported that β-catenin acts downstream of AKT signaling, as inhibition of AKT signaling attenuates the β-catenin expression level. And inhibition of both AKT and β-catenin attenuated A549 cells invasion. Furthermore, in the present study it was also found that AKT and β-catenin were downregulated in the miR-338-3p treated lung tumor. However, the mechanism underlying miR-338-3p modulating AKT and β-catenin signaling *in vivo* still needs to be investigated.

In conclusion, in the present study, miR-338-3p was validated as an inhibitor of lung cancer cell invasion via downregulation of AKT/β-catenin signaling. However, the

regulatory role of miR-338-3p in other signaling pathways and their underlying mechanism requires further investigation.

Acknowledgements

Not applicable.

Funding

The present study was funded by Heilongjiang Province Scientific Research Institution Innovation Grants (grant no. YC2016D002) and Harbin Scientific Research and Innovation Grants (grant no. 2015DB3AS010).

Availability of data and materials

The datasets used and/or analyzed during the current study are available from the corresponding author on reasonable request.

Authors' contributions

JL and TL designed the present study, performed the experiments, analyzed the data and wrote the manuscript. LC, NZ, YF, ZY, YL, CT and JH performed the experiments and analyzed the data.

Ethics approval and consent to participate

All procedures were performed with the approval of the Animal Ethics Committee of Shenzhen Jiake Biotechnology Co., Ltd. (Shenzhen, China).

Patient consent for publication

Not applicable.

Competing interests

The authors declare that they have no competing interests.

References

1. Siegel R, Naishadham D and Jemal A: Cancer statistics for Hispanics/Latinos, 2012. CA Cancer J Clin 62: 283-298, 2012.
2. Siegel R, DeSantis C, Virgo K, Stein K, Mariotto A, Smith T, Cooper D, Gansler T, Lerro C, Fedewa S, *et al*: Cancer treatment and survivorship statistics, 2012. CA Cancer J Clin 62: 220-241, 2012.
3. Siegel R, Naishadham D and Jemal A: Cancer statistics, 2012. CA Cancer J Clin 62: 10-29, 2012.
4. Wang X and Adjei AA: Lung cancer and metastasis: New opportunities and challenges. Cancer Metastasis Rev 34: 169-171, 2015.
5. Catela Ivkovic T, Voss G, Cornelia H and Ceder Y: microRNAs as cancer therapeutics: A step closer to clinical application. Cancer Lett 407: 113-122, 2017.
6. Chen X, Pan M, Han LL, Lu HT, Hao XW and Dong Q: miR-338-3p suppresses neuroblastoma proliferation, invasion and migration through targeting PREX2a. FEBS Lett 587: 3729-3737, 2013.
7. Baek SH, Ko JH, Lee JH, Kim C, Lee H, Nam D, Lee J, Lee SG, Yang WM, Um JY, *et al*: Ginkgolic acid inhibits invasion and migration and TGF-β-induced EMT of lung cancer cells through PI3K/Akt/mTOR inactivation. J Cell Physiol 232: 346-354, 2017.
8. Jiao D, Wang J, Lu W, Tang X, Chen J, Mou H and Chen QY: Curcumin inhibited HGF-induced EMT and angiogenesis through regulating c-Met dependent PI3K/Akt/mTOR signaling pathways in lung cancer. Mol Ther Oncolytics 3: 16018, 2016.
9. Meng J, Zhang XT, Liu XL, Fan L, Li C, Sun Y, Liang XH, Wang JB, Mei QB, Zhang F and Zhang T: WSTF promotes proliferation and invasion of lung cancer cells by inducing EMT via PI3K/Akt and IL-6/STAT3 signaling pathways. Cell Signal 28: 1673-1682, 2016.
10. Pan H, Jiang T, Cheng N, Wang Q, Ren S, Li X, Zhao C, Zhang L, Cai W and Zhou C: Long non-coding RNA BC087858 induces non-T790M mutation acquired resistance to EGFR-TKIs by activating PI3K/AKT and MEK/ERK pathways and EMT in non-small-cell lung cancer. Oncotarget 7: 49948-49960, 2016.
11. Hong-Yuan W and Xiao-Ping C: miR-338-3p suppresses epithelial-mesenchymal transition and metastasis in human nonsmall cell lung cancer. Indian J Cancer 52 (Suppl 3): E168-E171, 2015.
12. Zhang G, Zheng H, Zhang G, Cheng R, Lu C, Guo Y and Zhao G: MicroRNA-338-3p suppresses cell proliferation and induces apoptosis of non-small-cell lung cancer by targeting sphingosine kinase 2. Cancer Cell Int 17: 46, 2017.
13. Bos JL: Ras oncogenes in human cancer: A review. Cancer Res 49: 4682-4689, 1989.
14. Avruch J, Zhang XF and Kyriakis JM: Raf meets Ras: Completing the framework of a signal-transduction pathway. Trends Biochem Sci 19: 279-283, 1994.
15. Khosravi-Far R and Der CJ: The Ras signal-transduction pathway. Cancer Metastasis Rev 13: 67-89, 1994.
16. Mills NE, Fishman CL, Rom WN, Dubin N and Jacobson DR: Increased prevalence of K-Ras oncogene mutations in lung adenocarcinoma. Cancer Res 55: 1444-1447, 1995.
17. Pellegata NS, Sessa F, Renault B, Bonato M, Leone BE, Solcia E and Ranzani GN: K-Ras and P53 gene-mutations in pancreatic-cancer: Ductal and nonductal tumors progress through different genetic lesions. Cancer Res 54: 1556-1560, 1994.
18. Livak KJ and Schmittgen TD: Analysis of relative gene expression data using real-time quantitative PCR and the 2 (-Delta Delta C(T)) method. Methods 25: 402-408, 2001.
19. Jackson EL, Willis N, Mercer K, Bronson RT, Crowley D, Montoya R, Jacks T and Tuveson DA: Analysis of lung tumor initiation and progression using conditional expression of oncogenic K-ras. Gene Dev 15: 3243-3248, 2001.
20. Cai CL, Xie YX, Wu LL, Chen XJ, Liu HM, Zhou Y, Zou H, Liu D, Zhao Y, Kong X and Liu P: PLGA-based dual targeted nanoparticles enhance miRNA transfection efficiency in hepatic carcinoma. Sci Rep 7: 46250, 2017.
21. Tamura T, Kurishima K, Nakazawa K, Kagohashi K, Ishikawa H, Satoh H and Hizawa N: Specific organ metastases and survival in metastatic non-small-cell lung cancer. Mol Clin Oncol 3: 217-221, 2015.
22. Blandin Knight S, Crosbie PA, Balata H, Chudziak J, Hussell T and Dive C: Progress and prospects of early detection in lung cancer. Open Biol 7: 170070, 2017.
23. Lemjabbar-Alaoui H, Hassan OU, Yang YW and Buchanan P: Lung cancer: Biology and treatment options. Biochim Biophys Acta 1856: 189-210, 2015.
24. Tsai JH and Yang J: Epithelial-mesenchymal plasticity in carcinoma metastasis. Genes Dev 27: 2192-2206, 2013.
25. Shibue T and Weinberg RA: EMT, CSCs, and drug resistance: The mechanistic link and clinical implications. Nat Rev Clin Oncol 14: 611-629, 2017.
26. Linnerth-Petrik NM, Santry LA, Moorehead R, Jücker M, Wootton SK and Petrik J: Akt isoform specific effects in ovarian cancer progression. Oncotarget 7: 74820-74833, 2016.
27. Mundi PS, Sachdev J, McCourt C and Kalinsky K: AKT in cancer: New molecular insights and advances in drug development. Br J Clin Pharmacol 82: 943-956, 2016.
28. Tanno S, Tanno S, Mitsuuchi Y, Altomare DA, Xiao GH and Testa JR: AKT activation up-regulates insulin-like growth factor I receptor expression and promotes invasiveness of human pancreatic cancer cells. Cancer Res 61: 589-593, 2001.
29. Han J, Zhang L, Zhang J, Jiang Q, Tong D, Wang X, Gao X, Zhao L and Huang C: CREBRF promotes the proliferation of human gastric cancer cells via the AKT signaling pathway. Cell Mol Biol (Noisy-le-grand) 64: 40-45, 2018.
30. Enomoto A, Murakami H, Asai N, Morone N, Watanabe T, Kawai K, Murakumo Y, Usukura J, Kaibuchi K and Takahashi M: Akt/PKB regulates actin organization and cell motility via Girdin/APE. Dev Cell 9: 389-402, 2005.